

ted  $^{210}\text{Pb}$  in the part between 0.5 to 1 mm depth where  $^{210}\text{Pb}$  is missing. As the daughter products of  $^{226}\text{Ra}$  all have short half lives, this equilibration with  $^{210}\text{Pb}$  should be reached within about 100 years.

**K. COCHRAN** : If one looks at the data, published in Krishnaswami and Cochran (1978), it is apparent that the  $^{210}\text{Pb}$  is not in equilibrium with  $^{230}\text{Th}$  (in one nodule: C57-58-1,  $^{210}\text{Pb}$  in the top sample is 2505 dpm/g whereas  $^{230}\text{Th}$  is 725 dpm/g) and in all cases is considerably higher than the  $^{226}\text{Ra}$  activity.

The  $^{210}\text{Pb}$  deficiencies with regard to  $^{226}\text{Ra}$  at depth in the bottom and top sides of the nodules studied are produced by diffusion of  $^{222}\text{Rn}$  out of the nodule while resting on the sea floor. Since this is likely a continuous and probably a steady state loss, the  $^{210}\text{Pb}$  activity would be expected to reflect the  $^{222}\text{Rn}$  loss.

**C. LALOU** : If we accept that  $^{230}\text{Th}$  is a recent one as indicated by "exposure ages" would it be possible that instead of a diffusion of  $^{226}\text{Ra}$  it would be that  $^{226}\text{Ra}$  has had no time to reach equilibrium, and that this ratio may help to "date" the  $^{230}\text{Th}$ . It seems, from a rough calculation that there is a coincidence between the possible exposure age and the deficit in radium.

**K. COCHRAN** : This is a possible interpretation of the data. However, the observation of  $^{226}\text{Ra}/^{230}\text{Th}$  ratios higher than 2 at depth in the nodules strongly implies  $^{226}\text{Ra}$  migration. If this is the case, then ratios of  $^{226}\text{Ra}/^{230}\text{Th}$  lower than 1 (near the nodule surface-top side) are also probably due to radium diffusion. Then the use of  $\Sigma^{226}\text{Ra}/\Sigma^{230}\text{Th}$  for any chronological purpose is suspect. An extension of the argument like the one you are making is to interpret the deficiency of  $^{222}\text{Rn}$  (as indicated by  $^{210}\text{Pb}$ ) relative to  $^{226}\text{Ra}$  as due to time. This is consistent with an "exposure age" of a few days.

**K. BOSTROM** : In your talk you hinted out the possibility that Be and Th are about equally mobile in seawater when you discussed the supply of these elements to a nodule. But, wouldn't you expect Be to be much more mobile, that is, wouldn't that worsen your "Be-dilemma"?

**K. COCHRAN** : We tried to take into account the possibility that Be has a longer residence time, relative to Th, in sea water by correcting the  $^{10}\text{Be}$  exposure age accordingly. This does worsen the "Be-dilemma" if by that you mean the concordance of  $^{230}\text{Th}$ ,  $^{231}\text{Pa}$  and  $^{10}\text{Be}$  exposure ages, since the  $^{10}\text{Be}$  age increases and is even more disparate. This is one reason we feel there are problems with an "exposure age" approach.

**D. HEYE** : Even if I do not agree with your interpretations about "exposure time" and so on, I think that such radiochemical investigations are necessary from time to time. Such results will animate the alpha track daters (as I am) to clarify the possibilities and limits of their method and to look for control mechanism of their method, as I have shown them in Part II of my report.

As I remember, about 10 years ago, an intensive discussion was held about  $^{226}\text{Ra}$  diffusion in deep sea sediments in respect to the dating on using daughter products. Now this discussion is forgotten and datings are done with  $^{10}\text{Be}$  directly as well as with daughter pro-

ducts, too, using gamma spectrometry. Now this discussion rises anew and I think it would not be very effective to repeat it in the case of manganese nodules.

A last point, in figures 3 and 4, you have shown analysis of  $^{210}\text{Th}$ ,  $^{226}\text{Ra}$  and  $^{210}\text{Pb}$ . On the basis of these results an  $\alpha$ -decay and a decrease can be calculated. In figures 5a, 5b, 6a and 6b, there are given  $\alpha$ -tracks distribution and I think they do not correlate with the expected  $\alpha$ -ray decrease calculated from figures 3 and 4. Some discrepancies might be explained if a  $^{222}\text{Rn}$  diffusion was possible between your sample and the plastic counter.

**K. COCHRAN** : Your point is well taken. One of the conclusions of our work is that care must be taken in interpreting the alpha track profiles.

Regarding the  $^{230}\text{Th}$  dating of sediments using daughters such as  $^{226}\text{Ra}$  (determined by gamma spectrometry, for example), the well established process of  $^{226}\text{Ra}$  diffusion out of sediments has generally discredited such attempts unless 1) the sediments are accumulating fairly rapidly ( $> 1 \text{ cm}/1000 \text{ years}$ ) or 2) one neglects the data from the top few decimeters of the core, where most of the diffusion and  $^{226}\text{Ra}/^{230}\text{Th}$  disequilibrium occurs. Indeed, this part of the core may sometimes be lost in piston coring operations.

The alpha track densities calculated from the radium data agree with the measured track distributions except at the nodule surface. The reason for the discrepancy is the fact that the geometry of the nodule-track detector (film) arrangement is different at this point, and some alpha particles are not recoiled into the film directly under the nodule. This results in a lower than expected track density. The magnitude of such a loss depends on the experimental set-up and how the nodules are prepared for exposure. In addition, the radiochemical data are from larger sampling intervals than are the track density data and some smoothing of the calculated profiles would be expected. The improved resolution obtainable with the alpha track method was what led us to use this technique.

**F. YIOLU** : The isotopic ratio  $^{10}\text{Be}/^9\text{Be}$  is  $10^{-7}$  in nodules, ten times larger than  $^{10}\text{Be}/^9\text{Be} = 10^{-8}$  in sediments. Don't you think this speaks against a diagenetic origin of beryllium isotopes? This remark is made to point out the importance of measuring isotopic ratios, specially those of beryllium isotopes, in different terrestrial environments: sediments, nodules, sea-water, etc.; they may tell us something about the origin of beryllium in nodules.

**K. COCHRAN** : The ratio is different because sediments have more detrital  $^9\text{Be}$  (unaccompanied by  $^{10}\text{Be}$ ) than nodules. If anything, the difference tends to support a sea water origin for  $^{10}\text{Be}$  and  $^9\text{Be}$  in nodules. B.L.K. Somayajulu may wish to comment on this since his paper bears on the origin of Be in nodules.

**B.L.K. SOMAYAJULU** :  $^9\text{Be}$  is about 2 ppm in sediments and about 3-5 ppm in nodules an increase of a factor of 2 in the nodules.  $^{10}\text{Be}$  in the other hand is enriched by over a factor 5 in the nodules. Hence the specific activity in the nodules is higher than in the sediments. The reason for the low specific activity in sediments is due to the fact that there is a higher detrital  $^9\text{Be}$  content.

## TECHNO ENCRUSTATION PART I : RADIOMETRIC STUDIES.

C. LALOU (\*), T.L. KU (\*\*), E. BRICHET (\*),  
G. POUPEAU (\*), P. ROMARY (\*).

**ABSTRACT** - The distribution of radioactivities in a large polymetallic encrustation (TECHNO) sampled from the Pacific sea floor has been studied in great detail. The study includes measurements of the long-lived U and Th decay series isotopes, alpha-particle tracks and  $^{10}\text{Be}$  and  $^{26}\text{Al}$  (Results on the latter two cosmocnuclides have been reported by Guichard, Reyss and Yokoyama, 1978). The data are discussed in term of their implication on age dating of the sample. Two interpretations of the data are presented leading to vastly different time scales for the formation of the sample. Here the opinion is divided among the authorship. One group, as well as Guichard et al (1978), favors the million-years scale and the other favors scale measured in thousands of years. The principal pros-and-cons aspects of the two views are mentioned.

**RÉSUMÉ** - La répartition des éléments radioactifs dans une grande croûte polymétallique (TECHNO) provenant de l'Océan Pacifique a été étudiée en grand détail. Cette étude comprend les descendants à longue période des familles de l'uranium et du thorium ainsi que la répartition des traces alpha. Les cosmocnuclides  $^{10}\text{Be}$  et  $^{26}\text{Al}$  ont été mesurés antérieurement dans ce même échantillon par Guichard et al (1978). Les résultats sont discutés en fonction de leur implication pour la datation de cet échantillon. Deux interprétations des données sont présentées conduisant à des échelles de temps totalement différentes pour la formation de l'échantillon. Les avis sont partagés entre les auteurs, un groupe, de même que Guichard et al (1978) est en faveur d'une échelle de temps se mesurant par millions d'années, alors que l'autre est en faveur d'une échelle de temps se mesurant en milliers d'années. Les principaux arguments pour et contre ces deux opinions sont discutés.

## INTRODUCTION

TECHNO is a thick polymetallic encrustation dredged from 4020 m water depth at  $13^{\circ}09'S$  and  $148^{\circ}62'W$ , in Tapu Basin, which is located north of Tuamotu Ridge near the west end of Marquesas fracture zone (Figure 1). The general depositional environment near the sampling site can be inferred from Hoffert et al (1978) in their description of station 23 ( $13^{\circ}15'S$ ,  $148^{\circ}30'W$ , 4650 m) about 20 km to the southwest, and from reports on site 76 of DSDP (Shipboard Scientific Party, 1972). TECHNO is located at the base of a volcanic peak which may have been active recently. The coarse fraction of the sediment recovered at station 23 of Hoffert et al., includes phillipsite, palagonite, micronodules and some plagioclase and augite. In its silty fraction, phillipsite is the main constituent.

In this report, we present results of a detailed study on the long-lived isotopes of uranium, thorium and protactinium in the encrustation. In conjunction with data on the distribution of the cosmogenic nuclides,  $^{10}\text{Be}$  and  $^{26}\text{Al}$  (Reyss, 1977; Guichard et al., 1978), the results will be discussed in the context of their significance to age-dating of the specimen. Studies on the structural, mineralogical and chemical aspects of the encrustation are presented in a companion paper (Lalou et al., this volume).

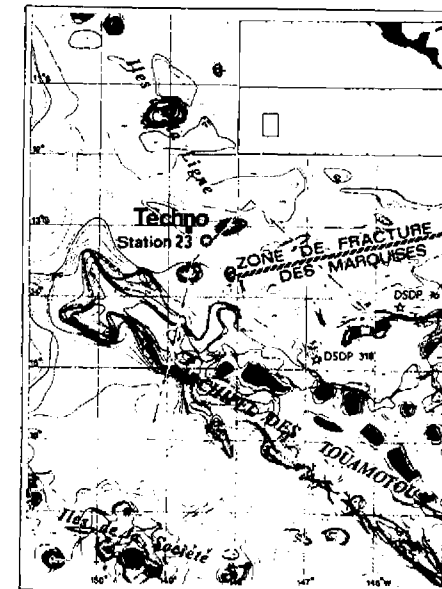


FIG. 1. - TECHNO location with reference to station 23 and DSDP 76 and 318 (map from Hoffert et al, 1978).

(\*) Centre des Faibles Radioactivités, Laboratoire mixte CNRS-CEA, 91190 Gif sur Yvette, France.

(\*\*) Department of Geological Sciences, University of Southern California, Los Angeles, California 90007, U.S.A.

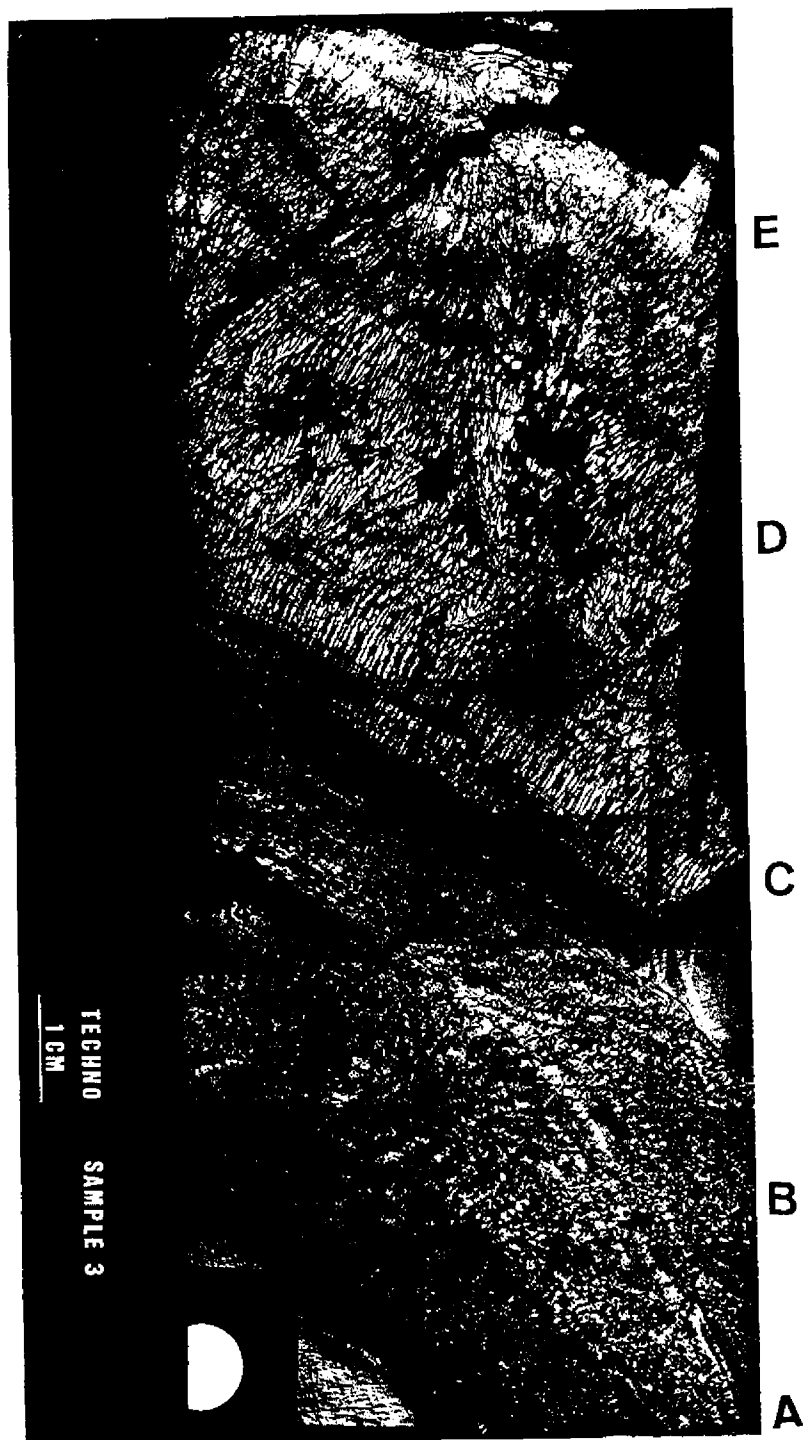


FIG. 2. - Oru-microphotography of a polished section of TECHNO (whole sample). Letters A through E denote zonations described in the text.

## SAMPLE DESCRIPTION

The specimen is about 15 cm thick and presents a total surface of about 1000 cm<sup>2</sup>. The principal Mn oxide constituent is  $\delta\text{MnO}_2$ . In a polished section (Figure 2), five zonations can be identified. From bottom to the top, they are:

Zone A - about 3 cm thick, with patches of white and brown material consisting mainly of organisms, feldspar and montmorillonite with some zeolite (phillipsite).

Zone B - 3 cm thick; brown oxide layer; contact with layers above and below sharp and being a zone for easy separation; montmorillonite, feldspar and goethite as principal crystalline constituents.

Zone C - 2.5 cm thick; similar in appearance as layer B except black in color; contact with zone D also sharp.

Zone D - dark brown layer of about 3.5 cm thick, with juxtaposed Fe-Mn oxides and an ochraceous mixture of goethite, apatite, feldspar and amorphous biogenic material.

Zone E - black Fe-Mn deposit, easily separated from zone D, about 2 cm thick.

Numerous fractures are present throughout the specimen, the surface of which is covered with thin films of montmorillonitic and illitic clays. This indicates that the fractures are developed *in situ* and may have been accentuated by air desiccation on land.

In this study, detailed radiochemical and alpha particle track measurements have been made on zone E. Analyses of uranium and thorium isotopes have also been performed on the deeper layers.

## EXPERIMENTAL

### (1) RADIOCHEMISTRY

Uranium and thorium-series isotopes are analyzed on nodule layers in a similar manner as described by Ku and Broecker (1969). The thickness (hence "depth") of each layer analyzed is estimated as follows. From a fixed, known area, successive layers are scraped off evenly and their weights (W) measured. After the last layer in the series is sampled this way, we measure the total thickness (T) scraped with a ruler read to better than 0.3 mm. The thickness of the *i*th layer (T<sub>*i*</sub>) is then calculated from:

$$T_i = \frac{W_i}{\sum W_i} \times T$$

Uranium and thorium isotopes are measured alpha spectrometrically using a <sup>232</sup>U-<sup>228</sup>Th spike. It is assumed that in the samples, <sup>232</sup>Th and <sup>228</sup>Th are in secular equilibrium. Protactinium-233, a beta emitter, is used as

a yield tracer for <sup>231</sup>Pa. The latter is counted either in a grid-chamber (at CFR) or in a low background windowless flow-type proportioned counter (at USC). The counting efficiencies of both counters are 50 %.

Part of the samples are measured at Gif and part at Los Angeles. In addition, several planchets of the prepared sources are counted using the facilities of both laboratories.

### (2) ALPHA TRACKS

A cellulose nitrate film produced by Kodak (LR 115) is used as the alpha track detector. The film is placed against a polished section of the encrustation. After an exposure time of about 6-8 months, the alpha particles tracks on the film are etched under controlled condition (2.5 N NaOH for 30 minutes at 60°C). The track density is measured with a scanning electron microscope (SEM). To study the fine alpha track distribution within the first millimeter of the encrustation, a photomosaic is made at  $\times 800$  magnification. Counting is performed along a 1.8 mm wide band, over successive depth ranges of 60  $\mu\text{m}$ . Below 1.1 mm depth, due to the small number of events, counting is done directly on the cathode screen of the SEM.

## RESULTS

Radiochemical measurements have been made on zone E for three vertical profiles (or series). Series (a) consists of 30 consecutive layers (from 0 to 15.3 mm) sampled from an 8.7 cm<sup>2</sup> area. Series (b) includes 12 successive layers taken from another area of the crust's surface whose area of scraping is 10.2 cm<sup>2</sup>. The depth range is 0-4 mm. Series (c) contains analyses made on splits used for <sup>10</sup>Be measurements (Guichard et al., 1978). The material is from an area of 425 cm<sup>2</sup>, sampled from surface down to a depth of 24 mm.

Results for the series (a) measurements are listed in Table 1, those for series (b) and (c) in Table 2. Uranium and thorium isotopes have also been analyzed for the deeper parts of the crust, on whole layers of zones A, B, C and D. These results are summarized in Table 3. In these and other tables, the uncertainties assigned are standard deviations ( $1\sigma$ ) based on counting statistics only.

The alpha particle track density measurements are made from two polished sections covering two contiguous regions in zone E: 0-6 mm and 6-15 mm. The results are shown in figure 4a. The total track density can be divided into two components. One component is due to <sup>230</sup>Th and its alpha emitting daughters and the other is due to (<sup>238</sup>U + <sup>234</sup>U) and the alpha emitters of the <sup>235</sup>U and <sup>232</sup>Th decay series. Since the

TABLE 1\*  
Radiochemical data of the series (a) measurements made on zone E

Layer N°	Depth interval (mm)	<sup>238</sup> U (ppm)	<sup>232</sup> Th (ppm)	<sup>234</sup> U/ <sup>238</sup> U (dpm/dpm)	<sup>230</sup> Th (exc) (dpm/g)	<sup>231</sup> Pa (exc) (dpm/g)	<sup>230</sup> Th (exc) (dpm/cm <sup>2</sup> )	<sup>231</sup> Pa (exc) (dpm/cm <sup>2</sup> )
1	0 - 0.22	13.8 ± 0.5	60 ± 12	1.12 ± 0.05	1951 ± 200	-	49 ± 5	-
2	0.22- 0.45	13.8 ± 0.3	35 ± 3	1.13 ± 0.03	531 ± 21	-	13.3 ± 0.6	-
3	0.45- 0.71	14.8 ± 0.6	24 ± 1	1.04 ± 0.05	40.2 ± 1.8	1.80 ± 0.17	1.57 ± 0.04	0.070 ± 0.007
4	0.71- 1.09	15.0 ± 0.4	37 ± 2	1.05 ± 0.03	46.5 ± 2.3	3.85 ± 0.3	2 ± 0.1	0.650 ± 0.013
5	1.09- 1.41	15.5 ± 0.5	29 ± 2	1.02 ± 0.04	63 ± 3.4	4.15 ± 0.4	2.2 ± 0.1	0.147 ± 0.014
6	1.41- 1.72	15.0 ± 0.4	31.5 ± 3.4	1.02 ± 0.03	19.3 ± 2.7	-	0.67 ± 0.08	-
7	1.72- 2.07	14.9 ± 0.5	25 ± 1	1.01 ± 0.04	19 ± 1.3	1.68 ± 0.27	0.75 ± 0.05	0.066 ± 0.011
8	2.07- 2.39	15.2 ± 0.6	27.1 ± 1.8	0.989 ± 0.046	27.8 ± 2.1	1.47 ± 0.35	1.02 ± 0.06	0.055 ± 0.013
9	2.39- 2.77	15.1 ± 0.8	26 ± 1	1.05 ± 0.07	5.9 ± 1.2	0.61 ± 0.09	0.23 ± 0.02	0.024 ± 0.003
10	2.77- 3.14	14.0 ± 0.5	36 ± 2.5	1.103 ± 0.045	13.8 ± 1.4	1.30 ± 0.99	0.39 ± 0.03	0.037 ± 0.028
11	3.14- 3.39	-	29 ± 1	-	-	-	-	-
12	3.39- 3.66	16.2 ± 0.8	28 ± 1	0.900 ± 0.048	6.0 ± 1.3	0.45 ± 0.28	0.16 ± 0.02	0.013 ± 0.008
13	3.66- 3.91	14.5 ± 0.9	30 ± 2	0.92 ± 0.07	11.1 ± 1.6	-	0.31 ± 0.06	-
14	3.91- 4.18	15.6 ± 0.5	27.0 ± 1.4	0.96 ± 0.03	7.47 ± 0.81	0.31 ± 0.05	-	-
15	4.18- 4.43	-	29.4 ± 2.1	-	-	-	-	-
16	4.43- 4.85	14.5 ± 0.7	23.0 ± 1.9	0.998 ± 0.056	-0.2 ± 0.12	-	-	-
17	4.85- 5.42	-	19.8 ± 1.8	-	-	-	-	-
18	5.42- 5.70	13.7 ± 0.5	21.1 ± 0.9	1.03 ± 0.04	5.46 ± 0.6	0.13 ± 0.07	-	-
19	5.70- 6.04	12.9 ± 0.4	21.1 ± 1.3	1.023 ± 0.036	2.7 ± 0.9	-	-	-
20	6.04- 6.35	14.0 ± 0.7	20.2 ± 1.9	1.008 ± 0.049	-0.5 ± 1.3	-	-	-
21	6.35- 6.87	12.8 ± 0.4	21.5 ± 1.3	0.966 ± 0.035	1.5 ± 0.8	-	-	-
22	6.87- 7.55	13.8 ± 0.7	18.7 ± 1.9	0.947 ± 0.049	0.9 ± 1.4	-	-	-
23	7.55- 8.29	13.8 ± 0.5	16.3 ± 0.9	0.962 ± 0.025	1.1 ± 0.8	-	-	-
24	8.29- 9.57	12.9 ± 0.7	16.2 ± 1.6	0.952 ± 0.048	0.4 ± 1.3	-	-	-
25	9.57-10.15	11.1 ± 0.4	12.6 ± 1.9	0.932 ± 0.034	0.5 ± 1.2	-	-	-
26	10.15-11.28	11.4 ± 0.5	11.9 ± 1.2	0.903 ± 0.041	-0.5 ± 0.9	-	-	-
27	11.28-12.33	10.2 ± 0.4	12.3 ± 1.7	0.975 ± 0.043	0.4 ± 1.1	-	-	-
28	12.33-13.29	10.1 ± 0.4	11.3 ± 0.9	0.956 ± 0.041	-0.4 ± 0.7	-	-	-
29	13.29-14.21	9.7 ± 0.4	12.3 ± 1.1	1.010 ± 0.048	1.3 ± 0.9	-	-	-
30	14.21-15.31	10.8 ± 0.8	12.7 ± 1.3	0.96 ± 0.08	-1.0 ± 1.3	-	-	-

\* Protactinium: samples 7 and 8 were measured and counted at Gif only whereas samples 12, 14 and 18 were measured and counted at Los Angeles only. The remainder of the samples were counted in both laboratories and the results generally agreed to within the counting errors, except for sample 10 (Gif:  $2.0 \pm 0.4$  dpm/g; Los Angeles:  $0.60 \pm 0.34$  dpm/g).

TABLE 2\*  
Radiochemical data of the series (b) and (c) measurements made on zone E

Layer N°	Depth interval (mm)	<sup>238</sup> U (ppm)	<sup>232</sup> Th (ppm)	<sup>234</sup> U/ <sup>238</sup> U (dpm/dpm)	<sup>230</sup> Th (exc) (dpm/g)	<sup>231</sup> Pa (exc) (dpm/g)	<sup>230</sup> Th (exc) (dpm/cm <sup>2</sup> )	<sup>231</sup> Pa (exc) (dpm/cm <sup>2</sup> )
1 bis	0 - 0.19	14.7 ± 0.7	46 ± 5	1.13 ± 0.05	2035 ± 113	145.5 ± 6.4	44.7 ± 2.4	3.20 ± 0.14
2 bis	0.19- 0.36	14.9 ± 0.6	23 ± 3	1.08 ± 0.04	661 ± 24	49.1 ± 2.1	13.7 ± 0.5	1.01 ± 0.04
3 bis	0.36- 0.61	15.5 ± 0.6	35.8 ± 1.5	1.06 ± 0.05	166 ± 5.5	8.31 ± 0.28	6.4 ± 0.2	0.251 ± 0.008
4 bis	0.61- 0.98	15.6 ± 0.6	34.6 ± 1.9	0.98 ± 0.04	60.4 ± 3.4	2.23 ± 0.13	3.9 ± 0.2	0.098 ± 0.005
5 bis	0.98- 1.31	14.9 ± 0.5	29.7 ± 1.8	1.10 ± 0.04	53.8 ± 2.9	3.05 ± 0.78	3.5 ± 0.2	0.120 ± 0.031
6 bis	1.31- 1.72	15.3 ± 0.4	32.5 ± 1.9	1.04 ± 0.03	24.0 ± 1.9	1.46 ± 0.20	2.7 ± 0.1	0.071 ± 0.009
7 bis	1.72- 2.07	14.3 ± 0.4	33.6 ± 1.7	1.04 ± 0.04	21.5 ± 1.4	-	1.5 ± 0.1	-
8 bis	2.07- 2.42	14.4 ± 0.5	29.0 ± 2.8	1.096 ± 0.044	17.9 ± 2.4	-	-	-
9 bis	2.42- 2.79	14.4 ± 0.6	29.7 ± 2	1.013 ± 0.055	26.0 ± 2.1	-	-	-
10 bis	2.79- 3.22	15.4 ± 0.7	29.1 ± 1.5	1.026 ± 0.053	14.1 ± 1.4	-	-	-
12 bis	3.69- 4.06	16.3 ± 0.4	26.8 ± 0.97	1.02 ± 0.028	4.3 ± 0.6	-	-	-
Ia	0 - 0.04	13.7 ± 0.6	38 ± 5	1.11 ± 0.06	1332 ± 73	-	6.6 ± 0.4	-
Ib	0.04- 0.2	14.5 ± 0.6	49 ± 7	1.16 ± 0.06	1669 ± 115	-	19.2 ± 1.3	-
II	0.2 - 0.7	14.9 ± 0.4	36.7 ± 2.5	1.034 ± 0.035	409 ± 19	-	30.4 ± 1.4	-
III	0.7 - 2	15.9 ± 0.6	32.0 ± 0.9	0.97 ± 0.04	91.0 ± 2.4	-	13.8 ± 0.3	-
IV	2 - 4	15.1 ± 0.4	30.0 ± 2	1.014 ± 0.034	10.8 ± 1.5	-	2.2 ± 0.3	-
V	4 - 7	15.2 ± 0.5	27.8 ± 1.6	0.993 ± 0.036	5.3 ± 1.0	-	2.3 ± 0.4	-
VI	7 - 12	13.8 ± 0.5	21.3 ± 2.3	0.97 ± 0.04	0.6 ± 1.3	-	-	-
VII	12 - 24	13.5 ± 0.3	15.6 ± 0.7	0.964 ± 0.028	1.6 ± 0.5	-	-	-

\* For Protactinium: chemical separations have been made at Los Angeles for samples 3 bis and 4 bis, for the 4 other samples they have been made at Gif. All samples have been counted in both laboratories and the results generally agreed to within the counting errors.

TABLE 3  
Radiochemical data for layers of zones A through D

SAMPLE	DEPTH (cm)	<sup>238</sup> U (ppm)	<sup>234</sup> U/ <sup>238</sup> U activ. ratio	<sup>234</sup> U (dpm/g)	<sup>230</sup> Th (dpm/g)	<sup>231</sup> Pa (ppm)
Zone D	2 - 5.5	10.5 ± 0.4	0.917 ± 0.039	7.1 ± 0.3	7.3 ± 0.3	8.1 ± 0.6
Zone C	5.5 - 8	10.9 ± 0.5	0.913 ± 0.049	7.3 ± 0.4	7.8 ± 0.3	5.1 ± 0.4
Zone B	8 - 11	7.3 ± 0.2	1.147 ± 0.039	6.2 ± 0.2	6.2 ± 0.3	8.3 ± 0.7
Zone A	11 - 14	4.1 ± 0.3	0.960 ± 0.075	2.9 ± 0.2	3.1 ± 0.3	3.7 ± 0.5

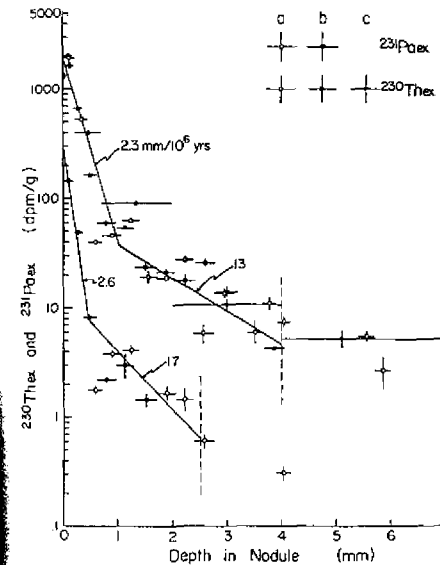


FIG. 3. - Depth plots of <sup>230</sup>Th<sub>ex</sub> and <sup>231</sup>Pa<sub>ex</sub> obtained from radiochemical analysis made in series (a), (b), and (c). For data points deeper than the dashed lines, only those differing significantly (outside ± 2σ from N<sub>ex</sub> = 0) are plotted. Average growth rate estimates are shown.

first component contributes mainly to the total tracks and is of geochronological interest (Heye and Beiersdorf, 1973; Andersen and Macdougall, 1977) a plot of this component is useful. This is done in figure 4c, in which tracks arising from the second component is subtracted from the total. The track density between 2 and 5 mm depth is taken to be the second component. It should be noted that below 4 mm, the alpha track density distribution is consistent with the one predicted from our radio-

chemically determined U and Th contents, assuming that each decay series is in secular equilibrium.

## DISCUSSION

### (1) GENERAL

To our knowledge, TECHNO has been subjected to the most detailed radiometric measurements on a single manganese concretion. The focus of our discussion will be on the time scale, or age, of formation of the specimen, based on the radiometric results. As a way of introduction, we summarize in the following the general depth distribution of the various isotopic signals that have been used for age-dating of nodules. These signals include excess <sup>230</sup>Th (<sup>230</sup>Th<sub>ex</sub>), excess <sup>231</sup>Pa (<sup>231</sup>Pa<sub>ex</sub>), <sup>234</sup>U/<sup>238</sup>U, alpha particle tracks, <sup>10</sup>Be and <sup>26</sup>Al. The most salient feature is their gross exponential (or quasi exponential) decrease with depth in zone E. In the deeper zones, A, B, C, D, <sup>230</sup>Th, <sup>234</sup>U and <sup>234</sup>U-<sup>238</sup>U are in secular equilibrium within experimental errors (with the possible exception for <sup>234</sup>U-<sup>238</sup>U in zone B: see Table 3) and <sup>10</sup>Be and <sup>26</sup>Al are below detection limits (Guichard et al., 1978).

Within zone E, the two relatively short-lived isotopes, <sup>230</sup>Th and <sup>231</sup>Pa, show the steepest concentration gradients: <sup>230</sup>Th<sub>ex</sub> decreases from about 2000 dpm/g at surface to zero at approximately 4 mm below and <sup>231</sup>Pa<sub>ex</sub> from a surficial value of about 150 dpm/g to near zero at below 2.5 mm (Tables 1 and 2). The alpha tracks show similar rapid decrease from surface to depth of 1-2 mm (Figure 4a).

The <sup>234</sup>U/<sup>238</sup>U ratio at top of the sample is close to that of sea water, about 1.14; it reduces to the secular equilibrium value of unity at 2-3 mm.

The concentration gradients of the two long-lived cosmogenic nuclides in zone E are more gentle: <sup>10</sup>Be

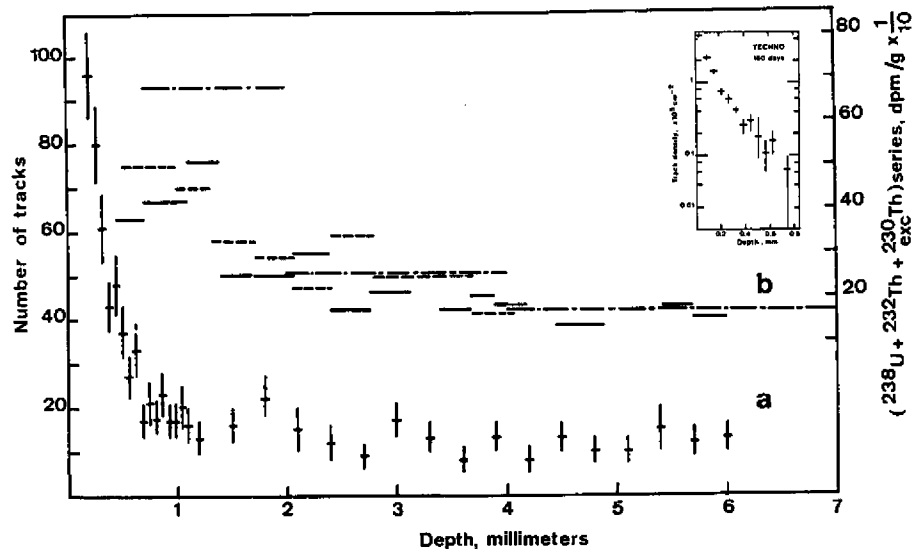


FIG. 4. — Distribution of U and Th series  $\alpha$  emitters with depth inside TECHNO  
 a: number of  $\alpha$  particle tracks measured in a cellulose nitrate detector exposed against a polished section of the Mn-rich crust.  
 b: total  $\alpha$  activity calculated from radiochemical data of  $^{230}\text{Th}_{ex}$ ,  $^{234}\text{U}$  and  $^{232}\text{Th}$  assuming that the daughters of each are at equilibrium.  
 c:  $^{230}\text{Th}_{ex}$  (and daughter products)  $\alpha$ -particle tracks density versus depth in the first millimeter of the crust.

decreases by a factor of 20 over a thickness of about 20 mm; the same magnitude of reduction is found for  $^{26}\text{Al}$  over a depth interval of 10 mm (Guichard et al., 1978).

Several additional observations are to be noted:

a) As shown in figure 3, the depth distribution of  $^{230}\text{Th}_{ex}$  and  $^{231}\text{Pa}_{ex}$  obtained from all three series (a, b and c) of analysis shows first-order agreement, indicating overall lateral homogeneity of the encrustation. However, sufficient differences exist in detail, and there are "reversals" in concentration gradient superimposed on the general decreasing trend with depth.

b) Although at about 4 mm below  $^{230}\text{Th}_{ex}$  is essentially reduced to nil (to within 2-sigma uncertainties), there are several exceptions, i.e., layers 18 and 19 in series (a) (Table 1) and layer V in series (c) (Table 2). A similar exception for  $^{231}\text{Pa}_{ex}$  below 2.5 mm is found in layer 14 of series (a) (Table 1)

c) A decreasing trend exists for  $^{232}\text{Th}$  from surface inward. At the base of zone E,  $^{232}\text{Th}$  is about three times less compared to the top of the zone. A less conspicuous decrease is shown by  $^{234}\text{U}$ . Both nuclides also show much lower levels in the deeper zones.

## (2) GROWTH TIME SCALE

Two schools of thoughts have been expressed toward relating the observed radioisotopes gradients to the age or growth rate of manganese nodules. One takes the

inward decrease as due to radioactive decay (e.g. Ku and Broecker, 1967; Krishnaswami et al., 1972). It assumes that during growth of the nodules, a fixed amount of radionuclides is incorporated into the growing layers. With time, the concentration of the nuclides in the layer diminishes as a result of decay. The other view hypothesizes that Mn concretions form very rapidly. Afterwards, they are exposed to the rain of radionuclides and experience almost no growth on the sea floor. The surface-adsorbed nuclides may penetrate inward, producing the observed concentration gradients via diffusion and/or mechanical mixing — both natural and artificial (during sampling) (e.g., Arrhenius, 1967; Lalou and Brichet, 1972). The data on TECHNO will be examined in light of these two alternative views. Unlike previous report on TECHNO (Guichard et al., 1978) this communication will not draw conclusion as to the preference of one view over the other, as no unanimous consensus exists among the authorship.

### (a) Interpretation based on decay.

Following Ku and Broecker (1967), the growth rates and their applicable depth range (in parenthesis) as obtained from the best-fitting logarithmic gradients of various isotopes in TECHNO are summarized as below:

- Based on  $^{230}\text{Th}_{ex}$  and  $^{231}\text{Pa}_{ex}$  (Figure 3)
- $^{230}\text{Th}_{ex}$ :  
 $2.3 \pm .8 \text{ mm}/10^6 \text{ yrs}$  (0-1 mm)  
 $13 \pm 7 \text{ mm}/10^6 \text{ yrs}$  (1-4 mm)

- $^{231}\text{Pa}_{ex}$ :  
 $2.5 \pm .9 \text{ mm}/10^6 \text{ yrs}$  (0-0.5 mm)  
 $17 \pm 10 \text{ mm}/10^6 \text{ yrs}$  (0.5-2.5 mm)
- Based on  $^{10}\text{Be}$  and  $^{26}\text{Al}$  (Guichard et al., 1978):  
 $\text{Be}$ :  $2.8 \pm .6 \text{ mm}/10^6 \text{ yrs}$  (0-20 mm)  
 $\text{Al}$ :  $2.3 \pm 1.0 \text{ mm}/10^6 \text{ yrs}$  (0-10 mm)
- Based on alpha tracks (Figure 4c) and assuming all tracks due solely to  $^{230}\text{Th}_{ex}$  and its daughters in equilibrium:  
 $0.8 \text{ mm}/10^6 \text{ yrs}$  (0-0.2 mm)  
 $2.5 \text{ mm}/10^6 \text{ yrs}$  (0.2-0.63 mm)
- Based on  $^{234}\text{U}/^{238}\text{U}$  ratio:  
 $\approx 2.5 \text{ mm}/10^6 \text{ yrs}$  (0-2.5 mm).

Considering the error limits involved and the range of depth intervals dealt with by the various isotopes, one notes a fair degree of internal consistency. In Table 4, ages at two selected depths calculated from interpolation of the average growth rates listed above for the various isotopes are compared. Though explicable by the data scatter and possible non-uniformity in growth rate, the trend of  $^{10}\text{Be}$ -based rate <  $^{230}\text{Th}$  based rate <  $^{231}\text{Pa}$ -based rate can also be attributed to a certain degree to the sampling artifact.  $^{10}\text{Be}$ , having the smallest gradient among the three nuclides, should be less vulnerable to any mixing or contamination effect during the layer-scraping procedure. That the  $^{231}\text{Pa}$  and  $^{230}\text{Th}$  may be too high is further suggested by the alpha track-data. This is best seen in a comparison of the radiochemical results with those of alpha track as shown in Figure 4 (a vs b). The presence of measurable  $^{230}\text{Th}_{ex}$  in Figure 4b between 1 and 4 mm is not reflected in the alpha track distribution. This may be explained only if in that depth range  $^{230}\text{Th}_{ex}$  is not accompanied by its daughters. Otherwise contamination or mixing during layer sampling is a distinct possibility.

It is obvious that, according to the above interpretation, the age of TECHNO is millions of years old. If we assumed that the total Mn-oxide thickness (11 cm) of TECHNO has deposited at a uniform rate despicted by

TABLE 4  
 Ages estimates based on interpolation of average growth rates calculated from various radioactivity gradients. The latter are assumed to be due to decay

Based on	Age ( $10^6$ yrs.)	
	at 2.5 mm	at 4 mm
$^{231}\text{Pa}_{ex}$	$0.32 \pm .28$ $.10$	
$^{230}\text{Th}_{ex}$	$0.55 \pm .37$ $.15$	$0.66 \pm .61$ $.19$
$^{10}\text{Be}$	$0.89 \pm .25$ $.15$	$1.43 \pm .39$ $.25$
$^{26}\text{Al}$	$1.09 \pm .83$ $.33$	$1.74 \pm 1.34$ $.53$
$^{234}\text{U}$	$\sim 1.0$	—

the  $^{10}\text{Be}$  data, the extrapolation would give an age of 40 m.y. for the sample. This is compatible with the age of 80 m.y. for the basement rock in the area (Pautot, pers. Comm.). There are several unanswered questions arising from the slow growth interpretation.

The first is the familiar question of why a 30 m.y. old object, weighing >10 kg has not been buried by the surrounding accumulating sediments. The sedimentation rate in the area is of the order of 2 - 4 m/ $10^6$  yrs (DSDP Shipboard Scientific Party, 1972; Ku et al., 1968). Hence in 30 million years 60 to 120 meters of sediments would have been accumulated.

Secondly, as pointed out earlier, unsupported activities of  $^{230}\text{Th}$  and  $^{231}\text{Pa}$  have been found in several instances below 4 mm. They are permissible only if one assumes that during that period higher growth rates accompanied by higher fluxes of  $^{230}\text{Th}$  and  $^{231}\text{Pa}$  than have been in more recent times occurred. The higher growth rates would contradict the  $^{10}\text{Be}$  results. At present, we cannot rule out the possibility of contamination, either during sample scraping or by material funneled in through natural fissures (Ku et al., 1975). It is estimated that admixture of less than 0.2 % of surface nodule material could account for the observed excesses, although it seems fortuitous to have similar contamination level at two different sampling areas (Figure 3). Future a track studies will be useful.

Thirdly, what causes the rather regular decrease of  $^{232}\text{Th}$  with depth? The three fold decrease obviously cannot be explained in terms of radioactive decay. Could this reflect change in growth rate or  $^{232}\text{Th}$  source input, or pure chance?

### (b) Interpretation based on diffusion or mixing:

Here the age ( $t$ , in years) of the entire encrustation is calculated from the total amount of a radionuclide,  $\Sigma N$  (in dpm  $\text{cm}^{-2}$ ), found therein and the production rate,  $P$ , (in dpm  $\text{cm}^{-2} \text{yr}^{-1}$ ), of that particular nuclide using the equation:

$$t = -\frac{1}{\lambda} \ln \left[ 1 - \frac{\lambda}{P} (\Sigma N) \right]$$

where  $\lambda$  = decay constant ( $\text{yr}^{-1}$ )

$\Sigma N = \int_0^z \rho C(z) dz$ ,  $z$  being the depth in sample  
 $C$  the concentration (dpm/g)  
 and  
 $\rho$  the sample density ( $\text{g}/\text{cm}^3$ )

For TECHNO,  $\Sigma N$  for  $^{230}\text{Th}_{ex}$  is 75 dpm/ $\text{cm}^2$ , and the production rate of  $^{230}\text{Th}$  (for a water depth of 4 km) is  $9.3 \times 10^{-3}$  dpm/yr. Hence, the age is 8,500 years. Similar calculations using  $^{231}\text{Pa}_{ex}$ ,  $^{10}\text{Be}$  and  $^{26}\text{Al}$  give ages of 6,300 years, 31,000 years and 20,000 years, respectively. These ages are younger than those based on the decay profiles by 3 to 4 orders of magnitude. The young ages serve to circumvent the problem of burial by sediment. Also the concept of inward diffusion-mixing of radionuclides (open system) may help to explain away such difficulties as presence of  $^{230}\text{Th}_{ex}$  and  $^{231}\text{Pa}_{ex}$  in

deep layers. However, this interpretation is not without debatable points. Some of them related to radiochemical aspects are put forth here.

First it is assumed that the radionuclides produced in the water column (for  $^{230}\text{Th}$  and  $^{231}\text{Pa}$ ) and in the atmosphere (for  $^{10}\text{Be}$  and  $^{26}\text{Al}$ ) are collected by the Mn encrustation with 100 % efficiency. This seems unlikely, as these isotopes are highly insoluble and they could be associated with various particulate phases throughout the water column, only a small portion of which would eventually be incorporated into the Mn encrustation. Manganese nodules covered by thin veneers of sediments are not uncommonly revealed by bottom photographs. The scenario that nodules grow only a fraction of their time on the sediment surface (Krishnaswami *et al.*, 1972) is a conceivable one.

Second, the young age, as well as the observation that most of the excess  $^{230}\text{Th}$  and  $^{231}\text{Pa}$  are confined to the surface few millimeters, would depict that the bulk of the specimen formed rapidly. One is inclined to question why should not disequilibria among  $^{238}\text{U} - ^{234}\text{U} - ^{230}\text{Th}$  and  $^{231}\text{Pa} - ^{235}\text{U}$  be found in the inner part of the specimen?

The third objection can be raised as to how the concentration gradients for the various isotopes can be generated in such a way that, to a first approximation, they are inversely proportional to the half-lives. The observed reversals in  $^{230}\text{Th}$  and  $^{231}\text{Pa}$  gradients mentioned earlier argue against the notion that the gradients are entirely caused by inward diffusion of nuclides from surface where they are adsorbed. Mechanical mix-in must also have played a part in generating the concentration profiles. There is no reason to expect such mixing-diffusion effect leads to much deeper penetration for  $^{10}\text{Be}$  and  $^{26}\text{Al}$  than for  $^{230}\text{Th}$  and  $^{231}\text{Pa}$ .

#### CONCLUDING REMARKS

Recent work of Ku *et al.* (1979) suggests that if diffusion of radioisotopes in nodules occurred, the effect could lead to even slower growth rates than those obtained strictly based on decay. Therefore, in the world of radiometric dating of manganese nodules, different ways of interpreting the same set of data can lead to age estimates that differ so greatly as to defy compromise. Clearly, one of the present two age interpretations must be in error by a wide margin. Or is it possible that both are wrong? Hopefully, the present paper will contribute toward future resolution of the problem.

#### ACKNOWLEDGEMENTS

T.L. Ku wishes to acknowledge the support of Commissariat à l'Énergie Atomique and the National Science

Foundation (OCE75-12960 and OCE77-04061). His stay at Centre des Faibles Radioactivités while this work was initiated was a most pleasant one.

For the French authors, this study has been partly supported by successive CNEOX and DGRST grants. It is a pleasure for us to recognize the good relations we have had with T.L. Ku, even when we scientifically disagree.

TECHNO sample has been given for study by L. d'Ozouville from CNEOX.

#### REFERENCES

- ANDERSEN M.E., MacDOUGALL J.D. (1977). - Accumulation rates of manganese nodules and sediments: an alpha track method *Geophys. Res. Lett.*, vol. 4, 351-353.
- ARRHENIUS G. (1967). - Deep sea sedimentation: a critical review of U.S. work. *Trans. Amer. Geophys. Union*, vol. 48, 604-631.
- GUICHARD F., REYSS J.L., YOKOYAMA Y. (1978). - Growth rate of manganese nodule measured with  $^{10}\text{Be}$  and  $^{26}\text{Al}$ . *Nature* 272, 155-156.
- HEYE D., BEJERSDORF H. (1973). - Radioaktive und magnetische Untersuchungen an Manganknollen zur Ermittlung der Wachstumsgeschwindigkeit bzw. zur Altersbestimmung. *Z. Geophys.*, vol. 39, 703-726.
- HOFFERT M., KARPOFF A.M., CLAUER N., SCHAAF A., COURTOIS C., PAUTOT G. (1978). - Neoformations et altérations dans trois faciès volcanosédimentaires du Pacifique Sud. *Océanologica acta*, 1, 1, 73-86.
- KRISHNASWAMI S., SOMAYAJULU B.L.K., MOORE W.S. (1972). - Dating of manganese nodules using beryllium 10. In: *Horn ed.: Ferromanganese deposits on the ocean floor*. Papers from a conference held at Lamont Doherty Geological Observatory, IDOE-NSF 117-122.
- KU T.L., BROECKER W.S. (1967). - Uranium, thorium and protactinium in a manganese nodule. *Earth Planet. Sci. Lett.*, vol. 2, 317-320.
- KU T.L., BROECKER W.S., OPDYKE N.D. (1968). - Comparison of sedimentation rates measured by paleomagnetic and the ionium methods of age determination. *Earth Planet. Sci. Lett.*, vol. 4, 1-16.
- KU T.L., KNAUSS K.G., LIN M.C. (1975). - An evaluation of dating nodules by the uranium-series isotopes. *Trans. Amer. Geophys. Union (EOS)*, vol. 56, 999.
- KU T.L., OMURA A., CHEN P.S. (1979). -  $\text{Be}^{10}$  and U-series isotopes in nodules from the central North Pacific. "Marine Geology and Oceanography of the Central Pacific Manganese Nodule Province". J.L. Bischoff and D.Z. Piper eds. 791-814. Plenum, N.Y.
- LALOU C., BRICHET E. (1972). - Signification des mesures radiochimiques dans l'évaluation de la vitesse de croissance des nodules de manganèse. *C.R. Acad. Sc. Paris, série D*, Tome 275, 815-818.
- LALOU C., BRICHET E., JEHANNO C. (1978). - TECHNO encrustation. Part II. - Structural and chemical study. This volume.
- REYSS J.L. (1977). - L'aluminium 26 empreinte du rayonnement cosmique pour le million d'années passées. *Thèse Doctorat d'Etat, Orsay*.
- SHIPBOARD SCIENTIFIC PARTY (1972). - Initial reports of the Deep Sea Drilling Project. Vol. IX, Papeete, Tahiti to Balboa, Panama, 3-20.

#### DISCUSSION

K. COCHRAN: If the crust you have studied was obtained from an outcrop, why would you necessarily expect it to be covered with sediment?

C. LALOU: Due to the general smooth topography (see map Figure 1) an outcrop being millions years old is very improbable.

K. COCHRAN: How do you explain the disagreement between the  $^{230}\text{Th}$ ,  $^{231}\text{Pa}$  and  $^{10}\text{Be}$  "exposure ages"?

C. LALOU: I have noted in the second part of this paper that it is an unsolved question, unless the geochemistry of Th, Pa and Be is not so identical as thought.

K. COCHRAN: The high alpha-track density you observe at the surface of the crust may be due to excess  $^{210}\text{Pb}$  and the rapid decrease in alpha-track density on 0-0.2 mm is an artifact.

C. LALOU: Excess  $^{210}\text{Pb}$  represents only one alpha particle then cannot enhance tremendously the alpha track count.

K. COCHRAN: If thorium ( $^{232}\text{Th}$ ) in nodules is derived from sea water you may see any pattern of  $^{232}\text{Th}$  with depth (increase, decrease,

constant or variable). This suggests that for nodules, the  $^{230}\text{Th}/^{232}\text{Th}$  ratio may be better to use than  $^{230}\text{Th}$  alone.

C. LALOU: If you can accept any profile for thorium 232 coming from sea water, while thorium 230 having the same origin and same geochemical behaviour would present only a radioactive gradient?

Y. YOKOYAMA: I wish to make a comment: I have measured  $^{238}\text{U}$  and  $^{232}\text{Th}$  activities with the non-destructive gamma-ray spectrometry. The  $^{238}\text{U}$  content ( $11.9 \pm 0.4$  dpm/g) of my measurements is in good agreement with your measurements by the alpha ray method ( $10.9$  dpm/g), but the  $^{232}\text{Th}$  activity, which was measured by us ( $3.4 \pm 0.1$  dpm/g) is about half of the  $^{232}\text{Th}$  activity measured by you ( $6.5$  dpm/g). Your measurements are made on several positions at the surface of TECHNO nodule, but mine are made on one point. Therefore, I should not generalize my results over all surface. Nevertheless, perhaps it suggests  $^{232}\text{Th}$  and  $^{230}\text{Th}$  are not in radioactive equilibrium. If it is so, the basic assumption that you used to the thorium isotope determination, mainly the radioactive equilibrium between the two nuclides,  $^{232}\text{Th}$  and  $^{230}\text{Th}$  is suspect.

C. LALOU: I know the difficulties inherent to the use of  $^{232}\text{Th}$  as a spike in alpha spectrometry. As I considered that the  $^{232}\text{Th}$  gradient with depth was important, I have verified it in two ways:

1) On some samples, we have made a double determination, one with the spike and the other without spike to verify that the equilibrium between  $^{232}\text{Th}$  and  $^{230}\text{Th}$  is achieved.

2) To verify the gradient, on five microlayers as it is indicated in the text and in Table 2 second part, we have measured  $^{232}\text{Th}$  by neutron activation analysis, we found values which are in good agreement with the one found at the same depth with radiochemistry and which confirm the gradient.

With these two verifications, we are sure of our measurements, and perhaps it is gamma ray spectrometric measurements which are suspect.